J Therm Anal Calorim (2012) 108:353–360
DOI 10.1007/s10973-011-1871-4

Loading of praziquantel in the crystal lattice of solid lipid nanoparticles

Studies by DSC and SAXS

Ana Luiza Ribeiro de Souza · Tatiana Andreani · Fernando M. Nunes · Douglas Lopes Cassimiro · Adélia Emília de Almeida · Clóvis Augusto Ribeiro · Victor Hugo Vitorino Sarmento · Maria Palmira Daflon Gremião · Amélia M. Silva · Eliana B. Souto

Received: 10 July 2011 / Accepted: 10 August 2011 / Published online: 3 September 2011

Abstract Praziquantel (PZQ) is the drug of choice for oral treatment of schistosomiasis and other fluke infections that affect humans. Its low oral bioavailability demands the development of innovative strategies to overcome the first pass metabolism. In this article, solid lipid nanoparticles loaded with PZQ (PZQ-SLN) were prepared by a modified oil-in-water microemulsion method selecting stearic acid as lipid phase after solubility screening studies. The mean particle size (Z-Ave) and zeta potential (ZP) were 500 nm and −34.0 mV, respectively. Morphology and shape of PZQ-SLN were analysed by scanning electron microscopy revealing the presence of spherical particles with smooth surface. Differential scanning calorimetry suggested that SLN comprised a less ordered arrangement of crystals and the drug was molecularly dispersed in the lipid matrix. No supercooled melts were detected. The entrapment efficiency (EE) and loading capacity of PZQ, determined by high performance liquid chromatography, were 99.06 ± 0.3 and 17.48 ± 0.05, respectively. Effective incorporation of PZQ into the particles was confirmed by small angle X-ray scattering revealing the presence of a lipid lamellar structure. Stability parameters of PZQ-SLN stored at room temperature (25 °C) and at 4 °C were checked by analysing Z-Ave, ZP and the EE for a period of 60 days. Results showed a relatively long-term physical stability after storage at 4 °C, without drug expulsion.

Keywords Solid lipid nanoparticles · Praziquantel · Differential scanning calorimetry · Scanning electron microscopy · Photon correlation spectroscopy · Modified oil-in-water microemulsion · High-shear homogenization

A. L. R. de Souza · A. E. de Almeida · M. P. D. Gremião
School of Pharmaceutical Sciences, Paulista State University, Araraquara, Brazil

A. L. R. de Souza · T. Andreani · A. M. Silva
Department of Biology and Environment, University of Trás-os-Montes e Alto Douro, P.O. Box 1013, 5000-911 Vila Real, Portugal

T. Andreani · A. M. Silva
Centre for Research and Technology of Agro-Environmental and Biological Sciences, Vila Real, Portugal

F. M. Nunes
Chemistry Research Centre, Chemistry Department, University of Trás-os-Montes e Alto Douro, Vila Real, Portugal

D. L. Cassimiro · C. A. Ribeiro
Institute of Chemistry, Paulista State University, Araraquara, Brazil

V. H. V. Sarmento
Department of Chemistry, Federal University of Sergipe, Itabaiana, SE, Brazil

E. B. Souto (✉)
Faculty of Health Sciences, Department of Pharmaceutical Technology, Fernando Pessoa University, UFP, Rua Carlos da Maia, 296, Office S.1, P-4200-150 Porto, Portugal
e-mail: eliana@ufp.edu.pt

E. B. Souto
Institute of Biotechnology and Bioengineering, Centre of Genomics and Biotechnology, University of Trás-os-Montes e Alto Douro (IBB-CGB/UTAD), Vila Real, Portugal

Introduction

Praziquantel (PZQ), [2-cyclohexylcarbonyl-1,2,3,6,711b-hydropypyrazine {2,1-a} isoquinolin-4-one], is the drug of choice for the treatment of most human trematode and cestode infections, being widely used in schistosomiasis, as well as in other fluke infections that are pathogenic to humans [1]. After oral administration, PZQ suffers a rapid and nearly complete absorption, to a significant first-pass effect, of liver metabolism and kidney elimination [2]. PZQ short half-life (0.8–1.5 h), poor solubility in water and low oral bioavailability make PZQ an excellent candidate for encapsulation in solid lipid nanoparticles (SLN) [3]. The aim of this study was the development and physicochemical characterization of PZQ-SLN. SLN have been reported as potential drug carriers to improve gastrointestinal (GI) absorption and oral bioavailability of poorly water soluble and/or lipophilic drugs [4–6]. SLN consist of a matrix composed of a lipid in the solid state at both room and body temperatures, usually stabilized with an emulsifying layer in an aqueous dispersion, and these particles usually show Z-Ave between 50 and 1000 nm [7]. These carriers are composed of physiological components and/or excipients of accepted status (e.g., GRAS status for oral and topical administration). This approach reduces the risk of acute and chronic toxicity [8]. Interaction and localization of PZQ into SLN composed of different types of solid lipids was conducted by differential scanning calorimetry (DSC) and small angle X-ray scattering (SAXS).

Materials and methods

Materials

PZQ was purchased from Henrifarma® (Brazil). The lipids and fatty acids used in this study were: stearic acid (SA; a C_{18} saturated fatty acid) provided by Acofarma (Portugal), cetyl palmitate provided by Sigma-Aldrich (USA), glyceryl behenate (Compritol® 888 ATO) and glyceryl palmitostearate (Precirol® ATO 5) gifted by Gatefossé (France), glyceryl tristearate (Dynasan® 118), glyceryl monostearate (Imwitor® 491), glyceryl stearates (Imwitor® 900) and hydrogenated coco-glycerides (Witepsol® E 75) were supplied by Sasol Germany GmbH (Germany). The emulsifier Poloxamer 188 (P-188) (Lutrol® F68) was provided by BASF ChemTrade GmbH (Germany). All other chemicals were of high analytical grade. Water used was of high purity (Milli-Q water with 18.2 MΩ cm).

Solubility studies of PZQ in solid lipids

The solubility of PZQ in eight different lipids was screened by mixing the drug at different concentrations (1, 5, 10 and 15%, w/w) with the respective lipid. The mixture was kept at 90 °C for 1 h for melting. The solubility was determined by visual parameters, after 30 min at 90 °C.

Preparation of SLN

The aqueous SLN dispersions were produced by a modified oil-in-water (o/w) microemulsion method using high-shear homogenization as described by Martins et al. [9]. Particles were composed of 5% (w/w) of solid lipid stabilized with 1% (w/w) of Poloxamer 188. Briefly, the solid lipid was melted at about 90 °C, and in parallel, in a separate beaker, Poloxamer 188 was dissolved in purified water and heated to approximately the same temperature. The hot lipid phase was poured into the hot water-phase under high-shear homogenization at 8000 rpm, for 10 min using Ultra-Turrax® T25 (IKA works). The obtained coarse emulsion was immediately dispersed in 10 mL of cooled distilled water (0 °C, in ice bath) followed by homogenization at 3400 rpm for 1 min. Subsequently, the dispersions were allowed to recrystallize under refrigerated temperature (about 4 °C, for 5 min) to obtain SLN and then (divided in two equal portions) stored at 4 °C and at room temperature. For the production of PZQ-SLN, 0.75% of drug was added to the melted lipid phase previously to the hot emulsification, following the same process as described above.

Preparation of binary mixtures of SLN components for thermal analysis

Binary mixtures of raw components, in the same ratio as figuring in SLN composition, were prepared by ground milling, namely SA and PZQ (SA/PZQ, 85:15); Poloxamer 188 and PZQ (P-188/PZQ, 2:1.5).

Analysis of mean particle size (Z-Ave), polydispersity index (PdI) and zeta potential (ZP)

The mean particle size (Z-Ave) and the PdI of SLN in the dispersion were assessed by photon correlation spectroscopy (PCS, Zetasizer Nano-ZS; Malvern Instrument, UK) at a fixed angle of 173° and a temperature of 25 °C. The ZP was measured by laser Doppler anemometry using the same instrument at the same temperature. The samples were diluted with distilled water before analysis. Each reported value was the average of three measurements.

Scanning electron microscopy (SEM) analysis

The morphology of SLN was analysed by SEM (JSM-7500F, JEOL, Japan), operating at an accelerating voltage of 2.0 kV, after coating the samples with gold using a sputter coater (JFC-1200 fine coater, JEOL, Japan). Before

analysis, the excess of water was left to dry at room temperature (25 °C) and subsequently glued on the stub.

Differential Scanning Calorimetry (DSC) analysis

DSC analysis was carried out in a Mettler DSC 1 apparatus (Mettler Toledo, Gieβen, Switzerland), and the melting enthalpy, onset and melting temperature were calculated by the STAR^e Software. The instrument was calibrated with indium and zinc. Analysis was performed under a nitrogen purge (50 mL min^{-1}). An empty standard aluminium pan (40 µL) was used as reference. About 4.0 mg sample was taken for analysis. DSC scans were recorded at heating rate of 10 °C min^{-1}. The samples were heated from 25 °C up to 160 °C. The crystallinity index (CI, %) of SLN was calculated applying the following equation, where ΔH stands for the melting enthalpy (J g^{-1}):

$$\text{CI}\ (\%) = \frac{\Delta H_{\text{aqueous SLN dispersion}}}{\Delta H_{\text{bulk material}} \times \text{Concentration}_{\text{lipid phase}}} \times 100. \quad (1)$$

Small Angle X-Ray Scattering (SAXS) analysis

SAXS measurements were performed at the Brazilian Synchrotron Light Laboratory (LNLS). The incident X-ray monochromatic beam ($\lambda = 1.488$ Å) was monitored with a photomultiplier and detected on a Pilatus detector (8 × 8 binning). The sample-to-detector distance covered a scattering vector q ranging from 0.20 to 6.0 nm^{-1}. The samples were placed in a cell at 25 °C between two Kapton sheets. The collimated X-ray beam was passed horizontally through a chamber containing the sample. Each SAXS pattern corresponds to a data collection time of 5 s. Silver behenate powder was used as standard to calibrate the sample-to-detector distance, the detector tilt and the direct beam position. The SAXS chamber parasitic scattering was also recorded (with bias and dark-noise subtraction) and subtracted from the sample pattern after sample attenuation correction.

Determination of entrapment efficiency (EE) and loading capacity (LC) by HPLC analysis

PZQ was analysed by a reversed-phase HPLC method (Dionex UltiMate 3000®, USA). The column was an ACE® 5 C18 (250 × 4.6 mm) with 5 µm particles. A mixture of 5% formic acid–methanol (30:70 v/v) was used as the mobile phase. The detection was carried out at 262 nm, with a flow rate of 1.0 mL min^{-1} and a sample injected volume of 50 µL. The column temperature was maintained at 25 °C. The calibration curve for the quantification of PZQ was linear over the range of standard concentration of PZQ from 20 to 100 µg mL^{-1} with a correlation coefficient of 0.999. The retention time of PZQ was about 6.1 min. Data acquisition was performed using chromatography software Chromeleon Chromatography Management System (CMS).

The EE was determined to assess the extent of PZQ incorporation in the nanoparticles. EE of PZQ-SLN was obtained by determining the concentration of the free PZQ against the total PZQ used in the formulation. Briefly, approximately 1 g of PZQ-SLN was weighted and then ultracentrifuged for 60 min at 4 °C at 35,000g (3K30, Sigma, Germany). The amount of PZQ in the supernatant was determined by HPLC. The EE and LC were calculated applying the following equations (Eqs. 2 and 3).

$$\text{EE}\ (\%) = \frac{\text{Total mass of PZQ} - \text{mass of PZQ in aqueous phase}}{\text{Total mass of PZQ}} \times 100 \quad (2)$$

$$\text{LC}\ (\%) = \frac{\text{Total mass of PZQ} - \text{mass of PZQ in aqueous phase}}{\text{Total mass of lipid}} \times 100. \quad (3)$$

Statistical analysis

Data were expressed as mean ± standard deviation, and were compared by analysis of variance (ANOVA). Differences were considered statistically significant at P value <0.05.

Results and discussion

The first step in formulating SLN dispersions is always the assessment of drug solubility in the lipid phase for the solubility studies. Eight lipids with different physicochemical properties were selected, as listed in Table 1. For the envisaged concentrations of PZQ most of them did not solubilise PZQ or only solubilise at 1% (w/w). As observed, the fatty acid SA solubilises the highest amount of PZQ (Table 1) and therefore it was selected to produce SLN due to its solubilisation properties and low cost.

The unloaded SLN depicted Z-Ave of 396.8 ± 2.8 nm and 505.6 ± 27.2 nm when loaded with PZQ. Both populations provided acceptable homogeneity in the size distribution, as indicated by the PdI value below 0.3 (Table 2). Regarding the ZP, SLN depicted a negative surface charge and the loading of PZQ did not significantly change the ZP of the particles. These absolute values were higher than 30 mV, suggesting a good physical stability since particle aggregation is not likely to occur owing to

Table 1 Results of lipid screening of PZQ in different solid lipids

Brand name of solid lipids	Chemical composition	Melting temperature/°C	g PZQ/100 g solid lipid			
			1%	5%	10%	15%
Precifac® ATO	Cetyl palmitate	43–53	−	−	−	−
Compritol® 888 ATO	Glyceryl behenate	69–74	−	−	−	−
Dynasan® 118	Glyceryl tristearate	70–73	−	−	−	−
Imwitor® 491	Glyceryl monostearate	66–77	+	−	−	−
Imwitor® 900	Glyceryl monostearate	54–61	+	−	−	−
Precirol® ATO 5	Glyceryl distearate	53–57	+	−	−	−
Stearic acid	Stearic acid	69	+	+	+	+
Witepsol® E 75	Hydrogenated coco-glycerides	38	−	−	−	−

+ Soluble; − PZQ crystals

Table 2 Mean particle size, PdI and ZP of unloaded and PZQ-SLN

Formulations	Z-Ave/nm	PdI	ZP/mV
Empty SLN	396.8 ± 2.8	0.156 ± 0.036	−33.5 ± 0.4
PZQ-SLN	505.6 ± 27.2	0.264 ± 0.044	−34.0 ± 1.1

electrostatic repulsion between SLN [10–12]. Furthermore, the use of steric stabilizer was also shown to produce stable formulations [13]. Poloxamer (P-188), a non-ionic emulsifier, is reported to decreases the electrostatic repulsion between the particles, it sterically stabilizes the nanoparticles by forming a hydrophilic coat around their surface [14].

The morphology of SLN was investigated by SEM. Unloaded SLN showed an anisometric shape with a cylinder-like irregular (Fig. 1). The incorporation of PZQ into SLN affected the morphology of the systems and spherical particles were produced, possibly because of the formation of a more homogenous lipid phase (Fig. 2).

The DSC provides information about the physical state and the degree of crystallinity of SLN matrices via thermal behaviour. Since, the advantages of SLN are essentially due to the solid state of the lipid matrix, the lipid crystallization is an important point for the performance of the SLN carriers both in vitro and in vivo [10, 15]. However, when less crystalline lipids are used for SLN production, the lipid matrix might not necessarily re-crystallize. A problem associated with the formation of supercooled melts is usually encountered when the preparation process is carried out by heat, such as during the preparation of SLN by melt emulsification or by hot o/w microemulsion method [16, 17]. DSC curves for bulk lipid, bulk Poloxamer-188, pure PZQ and physical mixtures are presented in Fig. 3.

The DSC analysis of bulk lipid, bulk surfactant and pure PZQ show a single sharp endothermic peak, with a maximum at 58.33, 54.00 and 141.17 °C, respectively (Fig. 3). In the PZQ-SLN, the drug was dissolved in the melted solid lipid. The physical mixture of PZQ and SA was analysed by DSC to assess a possible melting point depression of the lipid and to evaluate the crystalline character of the loaded drug. The ratios of PZQ to lipid were similar to that of weight ratios in the final SLN formulation. Since, the melting endothermic peak of PZQ around 141 °C was not recorded, the complete solubilisation of PZQ in the lipid matrix was then confirmed (Fig. 3d).

The DSC analysis of physical mixture P-188/PZQ was carried out to determine the interaction between the drug and the emulsifier, where a slight decrease of the melting peak at 128.50 °C and the reduction of the obtained enthalpy with respect to the expected value (Fig. 3e).

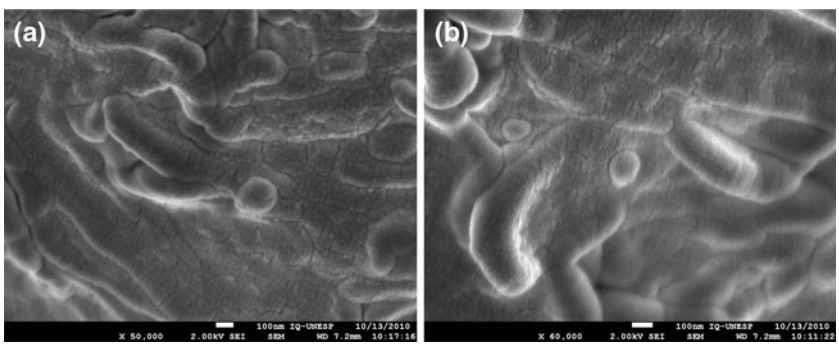

Fig. 1 SEM photomicrograph of unloaded SLN **a** ×50,000; **b** ×70,000

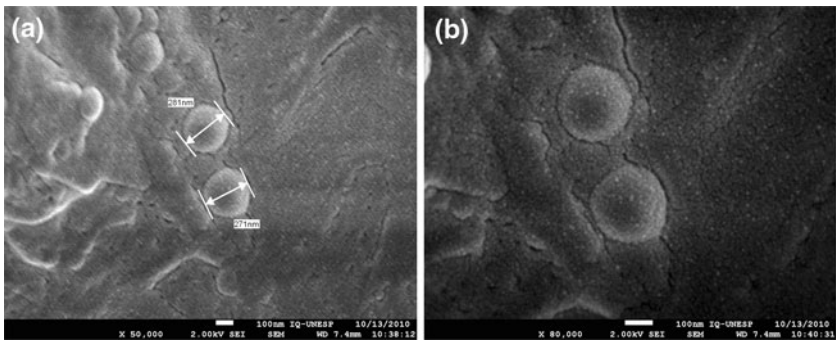

Fig. 2 SEM photomicrograph of PZQ-loaded SLN **a** ×50,000; **b** ×80,000

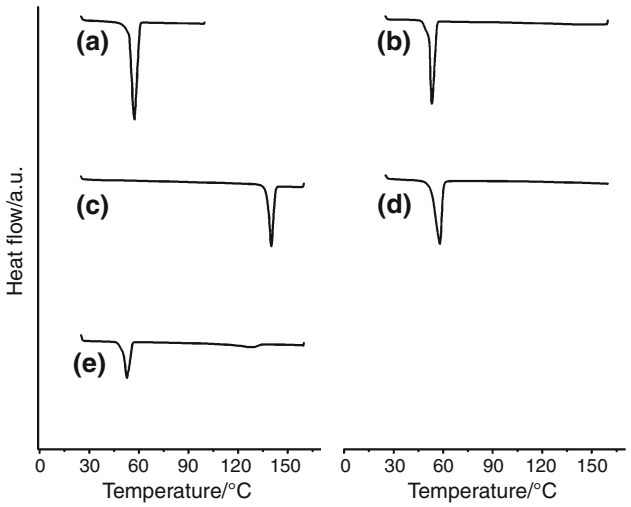

Fig. 3 DSC curves of *a* SA; *b* P-188; *c* PZQ; *d* SA/PZQ; *e* P-188/PZQ

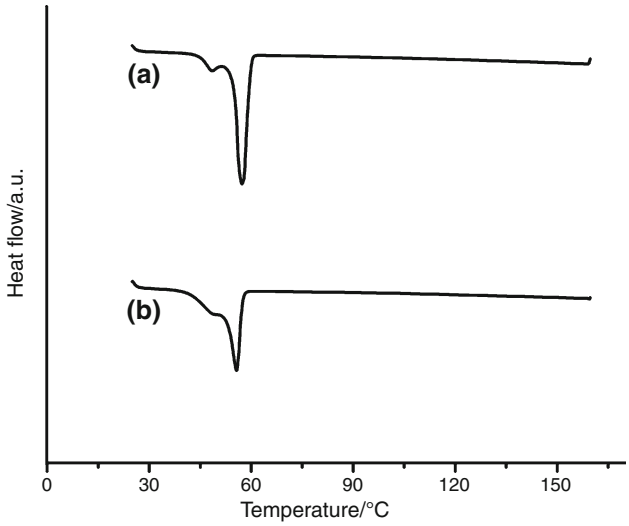

Fig. 4 DSC curves of *a* PZQ-unloaded SLN; *b* PZQ-loaded SLN

To produce SLN, the lipid is previously melted, following the dispersion in the hot aqueous phase. The obtained pre-emulsion is then homogenized to produce a hot o/w microemulsion. Cooling leads to crystallization of the lipid phase and the formation of SLN. This process means that, when analysing the SLN by DSC, the lipid has been melted before (drug dissolution process), i.e., DSC analysis of the SLN is a second melting process. When analysing the DSC curves of blank SLN (unloaded) and PZQ-SLN (Fig. 4a, b, respectively), broadening of the melting peak was observed with regard to the bulk SA and of the physical mixture. This result may be due to the nanometric size of the particles which had a large surface area besides a certain effect of the emulsifier molecules [18–20]. Moreover, a small endothermic peak was observed at 48.3 and 48.7 °C, respectively. This peak could indicate the presence of P-188 in the form of coating surrounding the particles. Similar result was observed by Aji Alex et al. [21]. No peak of PZQ at 141 °C was detected in DSC curves of PZQ-SLN compared with curves of raw material. No drug melting point may be attributed to the amorphous or molecularly dispersed structure of the PZQ in the lipid matrix. Similar results revealing that drug in the SLN were in amorphous state have also been reported [22, 23].

The melting enthalpy obtained for unloaded and PZQ-SLN had no significant differences, however, the unloaded SLN has higher amount of SA than PZQ-SLN. This fact can be due to the interaction of PZQ with P-188, even that weak, leading to a more structured particle in the presence of the drug, which was confirmed by SEM (Fig. 2). CI of the SLN was measured to eliminate the possibility of formation of supercooled melts [24–26]. The unloaded SLN showed a CI value of 86.4% whilst PZQ-SLN revealed a CI of 85.2%. The onset temperature and the melting point were above 40 °C, being the pre-requisite for SLN to remain in the solid state at body and room temperatures.

An average EE of 99.06 ± 0.30% and an average LC of 17.48 ± 0.05% were achieved for in the PZQ-SLN. The high value of EE may be due to the highly lipophilic nature of this drug and its high solubility in SA. The high EE of PZQ in the SLN can suggest a less ordered arrangement in

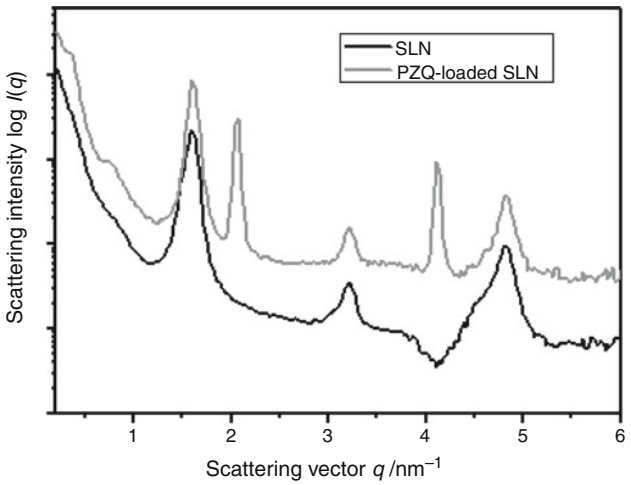

Fig. 5 SAXS patterns of (*black curve*) PZQ-unloaded SLN and (*grey curve*) PZQ-loaded SLN. The scattering profile is dominated by equally spaced Bragg reflections of integral order spacing indicative of one-dimensional lamella with a periodicity, *d*

the lipid structure and increased imperfections that allow incorporation of the drug molecules into the lipid matrix.

Figure 5 shows SAXS patterns of unloaded and PZQ-SLN. The magnitude of the scattering vector q is plotted against the logarithmic scattering intensity log $I(q)$. The SAXS pattern of unloaded SLN had three sharp peaks at 1.61, 3.21 and 4.82 nm^{-1} with same intervals (1.61 nm^{-1}) as depicted by the black curve. These peaks placed at periodic positions and with same intervals mean that the SLN prepared from SA had a lipid lamellar structure. Similar results were obtained by Lukowski et al. [27] and Maruyama et al. [28], who demonstrated by SAXS data that lipids such as cetyl palmitate and SA are arranged in a lamellar lattice structure.

The same SAXS pattern is observed to PZQ-loaded SLN (grey curve), however, the presence of the more two intensity peaks located at 2.1 and 4.2 nm^{-1} could be observed. These additional peaks suggest that the PZQ was incorporated into the lamellar structure of SA and this loading caused the formation of lamellar structures with two types of long spacing.

The distance between the lamellae, *d* could be determined the Bragg equation. The long spacing of lamellar structure was 3.90 nm, observed for SLN without PZQ. On the other hand, two types of long spacing in the PZQ-SLN were calculated to be 3.90 and 2.99 nm. This decrease in *d* values suggests that the PZQ interacted with the lipid matrix promoting the approach between lamellae which help understanding the drug effect on the morphology favouring the formation of spherical nanoparticles as observed in SEM images (Fig. 2). These observations confirmed the DSC results where no peak of PZQ at 141 °C was detected and that can be attributed to the effective incorporation of the PZQ (Figs. 3d, 4b; Table 3), and consequently increased EE.

It is known that the particle size distribution is one of the most important characteristic for the evaluation of the stability of colloidal systems. Optimized SLN formulations should display a narrow particle size distribution in the submicron range. Furthermore, particles greater than 1 μm and the increase of their number with the time can be an indicator of physical instability [29]. Thus, the particle size parameters were evaluated after 60 days of storage at 4 °C or at room temperature. Freshly prepared samples were

Table 3 DSC results of bulk materials and unloaded and PZQ-SLN

Samples	T_{peak}/°C	T_{onset}/°C	$\Delta H_{obtained}$/J g^{-1}	$\Delta H_{expected}$/J g^{-1}
SA	58.33	54.33	181.04	–
P-188	54.00	51.45	125.01	–
PZQ	141.17	137.69	90.80	–
SA/PZQ	58.67	52.55	140.31	153.88
P-188/PZQ	53.17/128.50	50.23/114.53	66.60/16.5	71.38/38.95
Empty SLN	48.33/58.17	45.91/55.01	125.64	170
PZQ-SLN	48.70/56.17	–	123.94	149

SA stearic acid; *P-188* Polaxamer 188; *PZQ* praziquantel; *ΔH* melting enthalpy

Table 4 Effect of storage time and temperature (4 °C or room temperature) on the mean particle size, PdI, ZP and EE dI, ZP of PZQ-SLN

PZQ-SLN	Z-Ave/nm	PdI	ZP/mV	EE/%
PZQ-SLN (0 day)	505.6 ± 27.2	0.264 ± 0.044	−34.0 ± 1.1	99.06 ± 0.3
PZQ-SLN 4 °C (60 days)	616.0 ± 26.5	0.335 ± 0.037	−28.9 ± 1.5	99.22 ± 0.1
PZQ-SLN RT (60 days)	1421.3 ± 208.8	0.903 ± 0.110	−28.2 ± 0.9	98.82 ± 0.3

divided in two batches, one left at room temperature and the other was placed at 4 °C. PZQ-SLN stored for 60 days at 4 °C showed a slight but significant increase of particle size ($P < 0.05$), when compared to the formulation immediately after production (Table 4). When stored at 25 °C for 60 days, the particle size showed a significant increase, ca. 2.3–2.8-fold, when compared to the initial formulation. The PdI follows the same variation as the particle size. Storage temperature did not significantly affect the ZP values, which were smaller than the measured on the day of production. The EE was not affected by the storage time. However, data indicates that storing the samples at 4 °C, the formulations still remained in their colloidal particle size range. These results suggest that the destabilization process was induced by increase of storage temperature, which increases the kinetic energy of the systems favouring particles collision [10]. Moreover, the particle growth generally precedes the gelling step [30]. In most cases, gel formation is an irreversible process, which involves the loss of the colloidal particle structure [13]. In this study, the gel formation was not observed.

During shelf life, rearrangement of the crystal lattice might occur in favour of thermodynamically stable configurations and this is often connected with expulsion of the drug molecules [10]. HPLC analyses for measuring the EE on day 0 and 45 days after preparation of PZQ-SLN showed no significant differences ($P > 0.05$), which anticipates that less ordered crystalline structures result in physical stability and little effusion of drug molecules from particles during storage time. Similar results were recently reported by Kheradmandnia et al. [31], for SLN containing beeswax and carnauba wax as lipid matrix for the incorporation of ketoprofen.

Conclusions

The SLN were produced using SA as lipid phase and the PZQ was successfully incorporated into SLN in the concentration of 15% in relation to lipid core. PZQ-SLN showed a mean particle size of 500 nm with narrow size distribution and high ZP value, indicating good physical stability. The morphology analysis showed that PZQ-SLN were of spherical shape. DSC measurements suggested that the drug was incorporated into SLN as solid solution, i.e., in molecularly dispersed form and the crystals of SLN were less ordered arrangement. Moreover, the PZQ-SLN remained in solid state. The high EE (99%) indicated a good compatibility between PZQ and the lipid core of SLN. SAXS measurements showed that SLN are consisted of a lipid lamellar structure and confirmed the effective incorporation of PZQ into SLN.

Acknowledgements Authors wish to thank Dr. Marcelo Ornaghi Orlandi and Tarek Fernandes for SEM analysis. *Laboratorio Nacional de Luz Sincrotron* (LNLS) is acknowledged and especially SAXS' staff support. Financial support provided by FAPESP (*Fundação de Amparo a Pesquisa*), CNPq (*Conselho Nacional de Desenvolvimento Científico e Tecnológico*) and CAPES (*Coordenação de Aperfeiçoamento de Pessoal de Nível Superior*) for Ana Luiza R. de Souza and by FCT (*Fundação para a Ciência e Tecnologia*) for Tatiana Andreani under the reference SFRH/BD/60640/2009 are acknowledged. The authors also acknowledge FCT under the reference PTDC/SAU-FAR/113100/2009.

References

1. Reynolds JEF, Parfitt K, Parsons AV, Swetman SC. Martindale the extra pharmacopoeia. 30th ed. London: The Pharmaceutical Press; 1993.
2. Ali BH. Short review of some pharmacological, therapeutic and toxicological properties of praziquantel in man and animals. Pak J Pharm Sci. 2006;19:170–5.
3. Mourão SC, Costa PI, Salgado HRN, Gremião MPD. Improvement of antischistosomal activity of praziquantel by incorporation into phosphatidylcholine-containing liposomes. Int J Pharm. 2005;295:157–62.
4. Das S, Chaudhury A. Recent advances in lipid nanoparticle formulations with solid matrix for oral drug delivery. AAPS PharmSciTech. 2011;12:62–76.
5. Muchow M, Maincent P, Muller RH. Lipid nanoparticles with a solid matrix (SLN, NLC, LDC) for oral drug delivery. Drug Dev Ind Pharm. 2008;34:1394–405.
6. Souto EB, Müller RH. Lipid nanoparticles—Effect on bioavailability and pharmacokinetics changes. In: Schäfer-Korting M, editor. Handbook of experimental pharmacology—Novel drug delivery approaches. vol. 197. Heidelberg, Berlin, Germany: Springer Verlag; 2009 (chapter 4). pp. 115–142.
7. Muller RH, Mader K, Gohla S. Solid lipid nanoparticles (SLN) for controlled drug delivery—a review of the state of the art. Eur J Pharm Biopharm. 2000;50:161–77.
8. Souto EB, Müller RH. Lipid nanoparticles (SLN and NLC) for drug delivery. In: Domb AJ, Tabata Y, Ravi Kumar MNV, Farber S, editors. Nanoparticles for pharmaceutical applications. American Scientific Publishers; 2007 (chapter 5). pp. 103–122.
9. Martins S, Silva AC, Ferreira DC, Souto EB. Improving oral absorption of Samon Calcitonin by mucoadhesive solid lipid nanoparticles (SLN). J Biomed Nanotechnol. 2009;5:76–83.
10. Mehnert W, Mader K. Solid lipid nanoparticles: production, characterization and applications. Adv Drug Deliv Rev. 2001;47:165–96.
11. Souto EB, Anselmi C, Centini M, Müller RH. Preparation and characterization of *n*-dodecyl-ferulate-loaded solid lipid nanoparticles (SLN®). Int J Pharm. 2005;295:261–8.
12. Souto EB, Muller RH. SLN and NLC for topical delivery of ketoconazole. J Microencapsul. 2005;22:501–10.
13. Heurtault B, Saulnier P, Pech B, Proust JE, Benoit JP. Physicochemical stability of colloidal lipid particles. Biomaterials. 2003;24:4283–300.
14. Schwarz C, Mehnert W, Lucks JS, Müller RH. Solid lipid nanoparticles (SLN) for controlled drug delivery. I. Production, characterization and sterilization. J Control Release. 1994;30:83–96.
15. Gonzalez-Mira E, Egea MA, Garcia ML, Souto EB. Factorial design study of ultrasound-engineered NLC for ocular delivery of flurbiprofen, Colloids Surf B Biointerfaces. 2010;81:412–21.

16. Bunjes H, Siekmann B, Westesen K. Emulsions of super-cooled melts—a novel drug delivery system. In: Benita S, editor. Submicron emulsions in drug targeting and delivery. Amsterdam: Harwood Academic Publishers; 1998. p. 175–204.
17. Ali H, El-Sayed K, Sylvester PW, Nazzal S. Molecular interaction and localization of tocotrienol-rich fraction (TRF) within the matrices of lipid nanoparticles: evidence studies by differential scanning calorimetry (DSC) and proton nuclear magnetic resonance spectroscopy (^{1}H NMR). Colloids Surf B Biointerfaces. 2010;77:286–97.
18. Westesen K, Bunjes H. Do nanoparticles prepared from lipids solid at room temperature always possess a solid lipid matrix? Int J Pharm. 1995;115:129–31.
19. Jenning V, Thünemann AF, Gohla SH. Characterisation of a novel solid lipid nanoparticle carrier system based on binary mixtures of liquid and solid lipids. Int J Pharm. 2000;199:167–77.
20. Doktorovova S, Araujo J, Garcia ML, Rakovsky E, Souto EB, Doktorovova S, Araujo J, Garcia ML, Rakovsky E, Souto EB. Formulating fluticasone propionate in novel PEG-containing nanostructured lipid carriers (PEG-NLC). Colloids Surf B Biointerfaces. 2010;75:538–42.
21. Aji Alex MR, Chacko AJ, Jose S, Souto EB. Lopinavir loaded solid lipid nanoparticles (SLN) for intestinal lymphatic targeting. Eur J Pharm Sci. 2011;42:11–8.
22. Chen H, Chang X, Du D, Liu W, Liu J, Weng T, Yang Y, Xu H, Yang X. Podophyllotoxin-loaded solid lipid nanoparticles for epidermal targeting. J Control Release. 2006;110:296–306.
23. Venkateswarlu V, Manjunath K. Preparation, characterization and in vitro release kinetics of clozapine solid lipid nanoparticles. J Control Release. 2004;95:627–38.
24. Kuntsche J, Westesen K, Drechsler M, Koch MH, Bunjes H. Supercooled smectic nanoparticles—a potential novel carrier system for poorly water soluble drugs. Pharm Res. 2004;21:1836–45.
25. Freitas C, Müller RH. Correlation between long-term stability of solid lipid nanoparticles (SLN^{TM}) and crystallinity of the lipid phase. Eur J Pharm Biopharm. 1999;47:125–32.
26. Bunjes H, Westesen K, Koch MHJ. Crystallinization tendency and polymorphic transitions triglyceride nanoparticles. Int J Pharm. 1996;129:159–73.
27. Lukowski G, Kasbohm J, Pflegel P, Illing A, Wulff H. Crystallographic investigation of cetylpalmitate solid lipid nanoparticles. Int J Pharm. 2000;196:201–5.
28. Maruyama T, Nakajima M, Ichikawa S, Sano Y, Nabetani H, Furusaki S, Seki M. Small angle X-Ray scattering analysis of stearic acid modified lipase. Biosci Biotechnol Biochem. 2001;65:1003–6.
29. Haskell RJ, Shifflett JR, Elzinga PA. Particle-sizing technologies for submicron emulsions. In: Benita S, editor. Submicron emulsions in drug targeting and delivery. Amsterdam: Harwood Academic Publishers; 1998. p. 21–98.
30. Freitas C, Müller RH. Effect of light and temperature on zeta potential and physical stability in solid lipid nanoparticle (SLN) dispersions. Int J Pharm. 1998;168:221–9.
31. Kheradmandnia S, Vasheghani-Farahani E, Nosrati M, Atyabi F. Preparation and characterization of ketoprofen-loaded solid lipid nanoparticles made from beeswax and carnauba wax. Nanomedicine. 2010;6:753–9.